

Fifth Quarterly Report

for

CHARACTERIZATION OF NICKEL-CADMIUM ELECTRODES

1 July, 1964 - 1 October, 1964

Contract No. NAS 5 - 3477

Prepared by

General Electric Company
Advanced Technology Laboratories
Schenectady, New York

for

Goddard Space Flight Center
Greenbelt, Maryland

\$ _____
GPO PRICE
\$ _____
OTS PRICE(S)
2.00
Hard copy (HC) _____
50
Microfiche (MF) _____

FACILITY FORM 602

N65 15814
(ACCESSION NUMBER)
42
(PAGES)
CR 60418
(NASA CR OR TMX OR AD NUMBER)

(THRU)
1
(CODE)
03
(CATEGORY)

Fifth Quarterly Report

for

CHARACTERIZATION OF NICKEL-CADMIUM ELECTRODES

1 July, 1964 - 1 October, 1964

Contract No. NAS 5 - 3477

Prepared by

General Electric Company
Advanced Technology Laboratories
Schenectady, New York

for

Goddard Space Flight Center
Greenbelt, Maryland

SUMMARY

15814

The objective of this contract is to develop a method of analysis and characterization of the electrodes used in nickel-cadmium sealed cells. It is based primarily on a comparison of detailed polarization measurements of single electrodes before and after periodic operation in selected modes of cyclic testing of cells at three temperature levels 00, 250, and 400C. A correlation of this data should provide a basis for specifying improved cells for space applications as well as comparing cells from various manufacturers.

During this quarter, Random Discharge tests (RA) and Constant voltage, Current limited Charging Cycling tests (RB) were continued. Shallow Discharge (CC) test electrodes were examined by x-ray diffraction, photo-micrography, electro-chemical capacity evaluation and recharacterization tests. Cells will be returned to CC test program next quarter as sealed cells. Examination of these and the other program plates will be completed next quarter.

Bulhan ↑

ERRATA SHEET
FIFTH QUARTERLY REPORT
FOR
CHARACTERIZATION OF NICKEL-CADMIUM ELECTRODES
CONTRACT NO. NAS5-3477
1 JULY, 1964 - 1 OCTOBER, 1964

<u>Page</u>	<u>Section</u>	<u>Line</u>	<u>Correction</u>
4	2.2	7	Table II instead of Table I
5	2.2	8	Table III instead of Table II
6	2.2.1	14	Table II instead of Table I
6	2.2.1	4	Table II instead of Table I
10	2.2.2	10	Table III instead of Table II
14	2.3.2	3	Table V instead of Table IV

TABLE OF CONTENTS

	<u>Page</u>
Summary	i
List of Tables	iv
1.0 Introduction	1
2.0 Discussion	4
2.1 Test Cell Assembly-Task II	4
2.2 CA-CB Test - Task IV	4
2.2.1 Characterization and Recharacterization of Nickel Electrodes from Shallow Discharge Cycling (CC) Test Cells	5
2.2.1.1. Test Results	6
2.2.1.2. 25°C Test Cells	6
2.2.1.3. 0°C Test Cells	9
2.2.1.4. 40°C Test Cells	9
2.2.1.5. 40°C Storage Tests	10
2.2.2 Characterization and Recharacterization of Cadmium Electrodes from Shallow Discharge Cycling (C-C) Test Cells.	10
2.2.2.2. 25°C Test Cells	10
2.2.2.3. 0°C Test Cell	11
2.2.2.4. 40°C Test Cells	11
2.2.2.5. 40°C Storage Tests	11
2.3 Shallow Discharge Cycling Tests-Task V	12
2.3.1.1. X-ray Diffraction Analysis of Positive Test Plates	13
2.3.1.2. Standard Plates	13
2.3.1.3. CC#4 Test Electrode P ₁ -27	13
2.3.1.4. CC#3 Test Electrode P ₁ -22	13
2.3.1.5. CC#5 Test Electrode P ₁ -45	14
2.3.1.6. CC#9 Test Electrode P ₁ -75	14
2.3.1.7. CC#7 Test Electrode P ₁ -91	14
2.3.1.8. CC#2 Test Electrode P ₁ -7	14
2.3.2. X-ray Diffraction Analysis of Negative Test Plates	14
2.3.3. X-ray Diffraction Analysis of Loose Material Adhering to Electrode Separators	15
2.3.4. Photomicrographic Study	15
2.3.4.1. Green (as-received) VO Plaque	16
2.3.4.2. Fully Charged VO Plaque	16
2.3.4.3. Fully Discharge VO Plaque	16

TABLE OF CONTENTS cont'd.

	<u>Page</u>
2.3.4.4. 0°C, CC#4 Test Electrode P ₁ -27	17
2.3.4.5. 25°C, CC#3 Test Electrode P ₁ -22	17
2.3.4.6. 40°C, CC#9 Test Electrode P ₁ -75	17
2.3.4.7. 40°C, CC#7 Test Electrode P ₁ -91	17
2.3.4.8. 40°C, CC#2 Test Electrode P ₁ -7	18
2.4 RA Test, Task IV	18
2.5 RB Test, Task VII	18
3.0 Program for Next Quarter	18
4.0 New Technology Report	18

LIST OF TABLES

	<u>Page</u>
Table I - Program Tasks	19
Table II - Characterization and Recharacterization Data on Positive CC-test Electrodes	20
Table III- Characterization and Recharacterization Data on Negative CC-test Electrodes	21
Table IV - X-ray Diffraction Data for Nickel CC-test Electrodes	23
Table V - X-ray Diffraction Data for Cadmium CC-test Electrodes.	24

LIST OF FIGURES

<u>Figure</u>		<u>Page</u>
1	Green Nickel Electrode 45X 2% Nital	25
2	P5-26 45X 2% Nital (Fully charged).	26
3	P5-25 45X 2% Nital (Fully discharged)	27
4	P1-27 45X 2% Nital.	28
5	P1-22 45X 2% Nital.	29
6	P1-75 45X 2% Nital.	30
7	P1-91 45X 2% Nital.	31
8	P1-91 5X 2% Nital.	32
9	P1-7 45X 2% Nital	33
10	P1-7 5X 2% Nital	34

1.0 INTRODUCTION

This report covers the work done during the fifth quarter of an 18-month program to develop a method for the analysis and characterization of the electrodes used in nickel-cadmium spacecraft batteries.

The goal of the program is to develop a correlation between detailed characterization data obtained on single electrodes in cells in various modes of cyclic operation. Such a correlation will provide a basis for specifying improved cells for space application and comparing cells from various manufacturers.

A breakdown of the program into tasks is given in Table I. The test program is divided into two parts: one, the initial characterization testing of plates (Task IV); and the other, the cycling of cells made from characterized plates in selected modes of operation (Tasks V - VII). Periodically, test cells will be removed from tests and the individual electrodes will be recharacterized and examined for changes in physical properties and comparisons made to the original characterization data.

The initial characterization will be made by analysis of data taken in single electrode experiments based on the use of continuous recording of charge-discharge curves under various testing regimes. The characterization information will include: 1) polarization of each electrode under various conditions, 2) complete charge and discharge curves showing electrode capacity, impurity levels, onset of gassing, graphitic and antipolar capacity, and reproducibility of cell operation, and 3) the onset of changes in capacity under various operation conditions.

Most plates in the program will be SAFT type VO, prepared as for space cells. Tests will be made at three temperatures: 0°, 25°, and 40°C. Failure analysis on cycled cells will be made, using visual, mechanical, chemical and electrochemical procedures.

During the fifth quarter, the Shallow Discharge Cycle test cells were examined visually and microscopically in cross section, by x-ray diffraction and by residual capacity determinations. Most of the positive plates exhibited extensive pimpling and were not returned to the cycling program.

These were replaced by a series of KO-15 plates which prior extended overcharge testing had shown to be less susceptible to pimpling than the SAFT VQ plates. Some of the SAFT positive plates were in "satisfactory" condition but were not returned to the testing program. None of the negative plates suffered obvious physical degradation and with a few exceptions, all were returned to testing program. Exceptions were those plates which were damaged in disassembly and those which were cut apart for x-ray examination.

The new Shallow Cycle test cells will be mounted in sealed cells fitted with pressure gauges and relief valves designed to vent excess pressure at 50 psi \pm 5%.

Investigation of the test electrodes of the Random Discharge Test cells and the Constant voltage, Current-limited Charge cycle test cells also showed pimpling of the positive plates. Some of these VO plate electrodes were replaced by KO-15 plates which had been characterized earlier. These cells were replaced in their respective cycling tests. The number of replacement electrodes were limited by the availability of reserve KO-15 plates that had been characterized earlier. The plates that were removed will be recharacterized and examined microscopically in the final quarter.

In the characterization of nickel hydroxide electrodes, a discharge plateau occurs at -0.200 volts (Figure 4, 1st Quarterly Report) which is designated as the graphitic capacity in our study. The name has been applied generally by workers in the field to this capacity, which historically was first observed in electrodes containing graphite in their structure. The capacity was ascribed to the formation of graphitic oxides on the surface of the graphite. However, since this capacity is observed in electrodes that do not contain graphite, as is true in this study, the name is misleading, and the graphitic capacity must be related in a more fundamental way to the operation of the nickel hydroxide electrode than was originally proposed. Because of the lack of a suitable substitute, the name graphitic capacity is retained, but with the understanding that it is not actually associated with the presence of graphite in the electrode structure.

Little work has been done on the cause or nature of the graphitic capacity. What little is known, points to the presence of some type of loose oxygen compound with the nickel substrate possibly an interstitial absorption of the oxygen in the nickel lattice at the surfaces of the nickel substrates. This is suggested by the fact that upon stand, a large part of the

charged graphitic capacity is lost; presumably by evolution of oxygen or by conversion to some other nickel compound.

A possible mechanism involving the graphitic capacity in the operation of the nickel hydroxide electrode is as follows: the graphitic capacity is partially charged during the initial stages of the charging of the electrodes; this would be expected in view of the lower potential needed. After some stage in the initial charging has been reached, the metastable compound formed would slowly evolve oxygen, possibly through the intervention of a catalyst on the nickel electrode surface. Upon overcharging the reaction relating to the graphitic capacity is converted to the oxygen evolution reaction, and the graphitic capacity becomes fully charged.

A consequence of this particular mechanism, coupled with the theory that the capacity is due to an interstitial compound of oxygen in the nickel lattice, would be that electrodes showing a large graphitic capacity could be subject to a more rapid destruction of the nickel substrate by overcharging than electrodes not showing the large capacity. This destruction arises from the fact that if oxygen is not evolved by the intermediate material at a relatively high rate as postulated in the charging mechanism given above, then it will enter the nickel lattice, and rupture it leading to mechanical destruction of the electrode. A partial correlation is given by the data in Table II, in which the electrodes that show mechanical degradation also in general show large graphitic capacities. This suggests that an examination of the data for plates that were discarded during the initial characterization should be made to check on this correlation. This will be done in the next quarter.

2.0 DISCUSSION

The work accomplished this quarter included disassembly of the Shallow Discharge Cycling test cells (Task V) and examination of electrodes, determination of residual charge capacity for one negative and one positive plate per cell followed by recharacterization of the fully discharged plates, and finally the microscopic and x-ray examination of one negative and one positive plate from each cell. In addition, the CC cells were reconstructed, using KO-15 electrodes as substitutes for the VO positive plates, as sealed cells.

Some positive electrodes were also replaced in the Random Discharge tests and in the Constant voltage, Current-limited Charging Cycling test.

The details of the work accomplished are reported in the following sections.

2.1 Test Cell Assembly - Task II

Shallow Discharge Cycling tests (Task V) in the previous quarters were conducted in vented cell assemblies. Water was added to the cells periodically to compensate for water lost by evaporation and by electrolysis. To prevent this loss and to force the oxygen recombination reaction at the negative electrode during the charge cycle, the reconstructed cells will be sealed. The new cells when inserted into the test program will be fitted with pressure gauges and relief valves to prevent rupture of the cells in the event of excessively high pressures.

In addition since all cells are in a series circuit, it was necessary to provide a simple by-pass switching circuit to permit any cell or cells to be removed from the cycle for any reason. At the end of this quarter the reconstructed cells were ready to be reinserted into the testing program.

2.2 CA-CB Test - Task IV

Initial characterization of positive and negative plates was completed in the fourth quarter. Plates removed from the Shallow Cycling test cells were recharacterized this quarter in an effort to identify the nature of or factors contributory to the loss of electrode capacity after extended periods of shallow cycling.

Table I is a compilation of the results of the original characterization and recharacterization tests subsequent to the Shallow Discharge Cycling test (CC) for the positive

plates. The CC test data (temperature; number of cycles), physical description of the electrodes and measurements of graphitic and nitrate reduction steps are also shown in the table. Finally, characterization and recharacterization of five positive plates (KO-15) which had been stored dry at 40°C without cycling for two months between tests are included.

Table II shows the results of the original characterization and recharacterization subsequent to the CC cycling test for the negative electrodes. The charge acceptance and the change of discharge capacity of the negative plates after the cycling test were also calculated and tabulated. Finally, four negative electrodes were stored in dry discharged state for two months at 40°C between characterizations to determine effect of the higher temperature on the discharge capacity of the negative plates without electrochemical activity.

One undischarged positive and one negative plate from each CC test cell were examined by x-ray diffraction to determine the qualitative nature of the materials in electrodes at each of three different depth planes. Photo-micrographs were taken of one each of the positive plates in the various test cells. The photos show an oblique cross-sectional view of the nickel plaques from the surface to the nickel plated steel substrate.

Details of the work done are given below.

2.2.1 Characterization and recharacterization of Nickel Electrodes from Shallow Discharge Cycling (CC) test cells.

Characterization data of all test electrodes were taken during previous quarters. The characterization process involved six consecutive cyclic charging and discharging of electrodes at pre-set current levels in separate test cells for pre-set time intervals. The half cell potentials of the positive and negative electrodes vs. a 10% discharged nickel electrode are continuously monitored and recorded during the cycling process. The length of time at constant current from the beginning to end of the charge and discharge reactions is converted into mahrs charge and discharge capacity. Six such measurements constituted the characterization and subsequent recharacterization of the individual electrodes for the purpose of this test.

The nominal capacity of the electrodes was determined to be approximately 1000-1200 mahrs for the nickel and 1200-1500 mahrs for the cadmium electrodes. The current and time requirements for the cycling program were adjusted to allow charge and discharge of these nominal capacities at various rates. The most commonly used program was a twelve hour charge at 140 ma and ten hours discharge at 160 ma with intervening rest periods of approximately 10 minutes.

In the case of the nickel electrode, there is no voltage inflection point during charge to signal completed charging (see Figure 4, 1st Quarterly Report). The discharge capacity, graphitic capacity and nitrate reductions capacity are readily obtained, however, and are recorded in Table I for several test VO electrodes.

In addition, data from several KO-15 electrodes which were characterized, stored in a dry discharged state for two months at 40°C, and recharacterized are included.

2.2.1.1 Test results

It was reported earlier that test cells CC#1-25°C and CC #6-0°C were found to be shorted out sometime during the Shallow cycling test period. For this reason, electrodes from these cells are not included in Table I.

2.2.1.2 25°C Test Cells

Of those electrodes run for 2660 cycles at room temperature (25°C), the plates in CC#3 were initially characterized at the C/10 rate while those in CC#5 were initially characterized at the C/1 rate. Electrodes in #3 cell showed a loss of capacity and also physical deterioration of the active material. In contrast, #5 cell electrodes showed a slight gain in capacity with no deterioration of material.

Earlier tests showed that in general, the higher the characterization charge rate, the fewer were the electrodes which survived the initial characterization without pimpling or blistering. This suggests that electrodes that survived the higher charge-rate characterization conditions may be, on the average, intrinsically more durable than those which have never been subjected to these conditions. Alternatively, it might be that the higher charge-rate alters the electrode in some way that it may be cycled for longer periods of time thereafter without deterioration. At any rate, the higher rate has served to screen out inferior electrodes from the standpoint of physical changes for the 25°C CC test cells. The importance of this effect is questionable in the case of the 0°C and 40°C test cells which will be described later.

The length of the graphitic step tends to increase during repeated cycles in the characterization process and appears to reach some final level. The graphitic step is believed to be associated with a reduction of absorbed oxygen. In a system without oxygen present, there will be no graphitic step. In the real case of a cycling cell, the amount of absorbed oxygen will be a function of the amount of oxygen generated by previous charges which is not consumed in subsequent discharges.

From these considerations, it can be seen that the first graphitic step at the end of the first discharge of the characterization program is indicative of both the nature of the electrode (its absorption capacity) and the prior history. The increase in subsequent steps are more probably due to some alteration of the electrode material during the characterization cycling itself. Only the final length of the graphitic step is important in the initial characterization data since this is most truly representative of the graphitic capacity of the electrode at the time the CC test started.

In the case of the recharacterization data, the first graphitic step is probably most significant. The fact that it is small compared with the previously measured values, suggests that little formation of graphitic capacity occurred in the latter portion of the CC program, and the initial graphitic capacity has been converted by lapse of time to regular capacity. The small initial length of the graphitic step supports the periodic observations that the cells were not inverted during the cycling.

CC #3 had an exceptionally high residual capacity of 1138 mahr. This cell inadvertently received two successive charges without an intervening discharge immediately before being removed from the test cycle program. While the error was unfortunate, it did tend to illustrate the importance of prior history on the length of the graphitic step. In spite of the inadvertent extra charge, the first graphitic steps (24, 50 mahr) were much lower than the final values (75, 130 mahr) developed during the recharacterization. Obviously one prolonged charge is not enough to develop the graphitic step and its transitory nature is reaffirmed.

Gassing behavior of positive electrodes has shed some light on the "memorization" phenomenon. It has been observed that charging efficiency of the positive electrode is a function of the state of charge of the electrode.

A consequence of this is that as the electrode is being charged from the fully discharged condition, the initial efficiency is high until roughly 40% of the capacity is restored. Thereafter the rate of evolution of oxygen steadily increases with increased charge level until the electrode is fully charged (see Figure 3, 4th Quarterly Report).

It is clear that the ratio of charge/discharge amp-hr. must be considerably higher to maintain a high level of residual capacity over an extended period of Shallow discharge cycling than would be required if the electrode was fully discharged. The precise ratio is difficult to determine since the rate of oxygen evolution changes with increasing charge level. Moreover, both the slope and onset of the gassing curve also varies with charge rate and cycling history of a particular plate. Finally, in addition to the spread between individual samples, there is a temperature and concentration effect.

In view of these considerations, it is not surprising that the residual capacity of the test plates has been found to be spread over a range of 20-30% of the nominal electrode capacity.

The 1138 mahr capacity of P₁-23 is inexplicable, however, at this point. Presumably the true residual capacity was of the order of 200-400 mahr before the extra 300 mahr charge that it received before being removed from the test program.

The nitrate reduction steps appeared only after several voltage inversions during the recharacterization process. This was to be expected if there was little or no inversion during the CC test cycling. Under such conditions, nitrate pockets not exposed and reduced during cleaning and characterization will remain inaccessible to electrochemical reaction until a sequence of deep discharges uncover them. The fact that the nitrate reduction was still visible at all after the prolonged cycling history illustrates the permanence of nitrate contamination of the positive electrodes. It also underscores the necessity of thorough electrochemical cleaning of positive plates made by nitrate impregnation prior to cell assembly.

22.1.3 0°C Test Cells

The residual capacity of one positive electrode in the test cell which did not develop an internal short circuit during the CC test was found to be very low. The change in characterized capacity, however, was very slight (approx. 5%) from the recharacterization data. Measurements of the graphitic steps and nitrate reduction steps indicates there was little or no voltage inversion. This indicates that this particular electrode was supplying only a small fraction of the total cell capacity during the CC test since there was sufficient cell capacity to prevent cell inversion.

It further illustrates the importance of running residual capacity checks on all electrodes in a cell in future tests. The physical appearance of the electrode indicated some loss of material from this electrode. The capacity determined by the recharacterization demonstrates that some previously unavailable capacity must have been developed during the CC test cycling. This probably resulted from corrosion of the sintered nickel structure and is consistent with similar observations by other experimentors.

2.2.1.4 40°C Test Cells

The electrode tested from CC#9 was found to have lost capacity--presumably due to loss of material from the electrode. Residual capacity was not measurable in spite of the fact that the cell had an open-circuit potential of greater than 1 volt immediately after being removed from the CC test program. All cells except CC#3 were removed at the same time but disassembled only immediately before the residual capacity checks were made. The appearance of the electrode suggests the possibility of a high resistance internal short that might have discharged this cell slowly in the interium period. Both the small initial graphitic and nitrate reduction steps seem to indicate that the cell had been functioning normally without repeated inversions in the latter portion of the test period.

The same observations apply to CC test cell #2. The low graphitic steps on recharacterization should be noted. This shows that the graphite step appears to be converted to permanent capacity and that the new graphitic capacity is not developed without extensive overcharge.

There was no obvious change in electrode appearance showing that loss of initial capacity is not necessarily due to loss of material from the electrode. Moreover the test temperature effect on decomposition of charged material was not the reason since the residual capacity was quite high compared with the 25°C test cells. There is undoubtedly some long time affect of temperature but the present data is not in itself conclusive. Graphitic and nitrate reduction steps indicate again that cycling was not accompanied by extended periods of potential inversion.

2.2.1.5 40°C Storage Tests

The 40°C CC test cells discussed above were cycled for 53 days. A separate group of KO-15 plates, essentially the same as the VO plaques, were characterized, stored at 40°C in a dry discharged state for 60 days and recharacterized. There was no significant change in capacity, appearance, graphite step or nitrate reduction step. 40°C temperature alone does not affect electrode capacity of KO-15 or VO plates, by analogy--over the test period.

2.2.2 Characterization and Recharacterization of Cadmium Electrodes from Shallow Discharge Cycling (C-C) Test Cells.

Characterization of all test electrodes was done in previous quarters. Half cell potentials (with respect to 10% discharged nickel reference electrodes) were recorded as a function of time and current. Charge and discharged capacities respectively are measured by converting the length of voltage traces to points of inflection and converting to mahr capacity figures. Six such measurements constituted the characterization and subsequent recharacterization for the purpose of this test. The pertinent data is recorded in Table II.

In the case of the negative electrodes, there is a pronounced inflection point at the completion of the charging reaction (see Figure 4, 1st Quarterly Report). It was possible to measure both the charge acceptance and discharge capacity and calculate and tabulate the percent of charge acceptance. In some cases, there is shown to be a greater than 100% charge acceptance. The power supplies used showed some tendency to increase current over a period of several days because of improper ventilation in the equipment. This was particularly true for the first of a series of characterization tests when several batches of electrodes were characterized in close consecutive order. The last electrodes to be characterized (eg. N-121-N-124, Table III) were more carefully controlled and the data more dependable in this respect. The charge acceptance here was found to be 85-95% with an average discharge capacity of 1350 mahr.

2.2.2.2 25°C Test Cells

CC#3 received an inadvertent extra charge prior to being removed from the CC test program. Residual capacity of the two tested electrodes is therefore, meaningless. The decrease of discharge capacity of these electrodes varied from 0-17% over the period of the test as determined by recharacterization. The % charge acceptance from the original characterization might be anomalously high. The recharacterization (when the power supplies were more carefully monitored) tend to support the original figures of 95-100%, however.

Discharge capacity of electrodes in CC #5 increased from 20-30% over the duration of the test period. This is probably not correct, however, since the original characterization done at the C/1 rate showed inordinately low capacities. The % charge acceptance in the original characterization illustrates the unacceptability of these figures since all are consistently greater than 100%. The % charge acceptance in the recharacterization data is more dependable. The residual capacities were found to be about the same as the positive electrodes in this cell and close to the 250 mahrs discharge portion of the test program cycle. There was no measurable anti-polarity charge on either characterization or recharacterization of any of these electrodes.

2.2.2.3. 0°C Test Cell

N₁-26 from CC#4 showed a slight increase of discharge capacity (+2.8%) at the completion of the cycling test. No significant change in charge acceptance was found from the characterization and recharacterization data (97, 98% respectively). The residual charge capacity (781 mahrs) was about 55% of the nominal capacity (1400 mahrs). There was no measurable change in the carbonate step nor the anti-polaric charge step.

2.2.2.4. 40°C Test Cells

Residual charge values of electrodes P₁-72, 50, 10 (CC#'s 9, 7, 2, respectively) were 763, 583, 538 mahrs covering a range of 60-45% of the nominal capacities. Discharge capacity of N₁-72 (CC#9) dropped slightly from beginning to end of the test period. N₁-50 appeared to have gained in discharge capacity but this affect is probably not real as has been explained earlier. The apparent lack of capacity loss at the higher temperature is in marked contrast to the electrodes in the Room Temperature cell CC#3.

2.2.2.5. 40°C Storage Tests

Four of the cadmium test electrodes were stored for two months after characterization and subsequently recharacterized. The electrodes were stored in the dry discharged condition (as were the positive counterparts) and yet all lost discharge capacity as a result of the storage. There was no change in the antipolarity charge step nor the carbonate step in these just as was the case in all other cadmium electrodes tested. There was no apparent change in % charge acceptance -- all ranged from 85-90%.

2.3 Shallow Discharge Cycling Tests - Task V

In addition to the recharacterization of CC test cell plates described in the previous section, one positive and one negative electrode from each test cell was checked by x-ray diffraction and photo-micrography.

X-ray diffraction patterns from 40° - 45° 2θ using $\text{CuK}\alpha$ radiation (Zr filter) with a GE x-ray Diffraction Analysis machine were taken of one each of the positive and negative plates from each CC cell. These electrodes were kept in the cells until just prior to the analysis. Drying the nickel electrodes in the charged condition in dry, deoxygenated nitrogen at room temperature did not affect the residual capacity. Drying the cadmium plates under the same conditions, however, made approximately 30% of the capacity temporarily inaccessible. To prevent the possibility of artifact formation giving spurious results on the diffraction patterns, all samples were sealed wet and unwashed in 0.5 mil Profax film.*

Initially it was hoped that the x-ray diffraction tests might be done on three successive levels within the active material. This was to be accomplished by abrading away the covering material after examining the first and second levels. The attempts were unsuccessful because of the difficulty of controlling the depth of the abraded "cuts" but more important, because of "smearing" of the active material into the open pore structure. Attempts to "pot" the plates in epoxy resin and grinding away the surface as in metallographic preparation introduced an extremely high background that obscured all but the strongest characteristic peaks. Finally, it became evident when a few successive analyses were run of the surfaces of successive plates, that the structure of the electrode varied considerably from one sample to another without regard to handling or electrochemical cycling history.

X-ray diffraction analysis was also run on the nylon separator material to determine unequivocally the nature and source of black material remaining after cells were disassembled.

Micro-photographs of the cross section of one of each of the positive test electrodes were made. These photos are reproduced and discussed in more detail, below, together with a discussion of the information derived from the x-ray analysis.

* Biaxially oriented polypropylene film from Hercules Powder Co.

2.3.1.1 X-ray Diffraction Analysis of Positive Test Plates

Initially several electrodes were fully charged and fully discharged by connecting several cells with only nickel plates in series connection with a power supply. A constant current of 250 ma. was applied for 10 hrs. so that the positive plates were fully charged and the nickel counter electrodes fully discharged. Peak heights are shown in Table IV for fully charged and fully discharged plates of one pair of samples. The values listed are of particular samples and are typical of, but not identical to, other samples in the same charge condition. Absolute values are roughly proportional to the surface composition of the examined area. These vary, of course, from sample to sample, and to a lesser degree, from one area to another on the same plate.

Even peaks of different planes of a particular species vary because of random variations in crystal orientation. Since it was hoped that the nickel powder matrix would serve as an internal standard of peak height comparative heights, these considerations were devastating to the success of this venture. Nevertheless, some tentative conclusions could be reached on the basis of the experimental data.

2.3.1.2 Standard Plates

It was immediately evident from examination of the diffraction charts that there were no unusual compounds in major proportions on the surface of the plates. In the case of the fully charged plates, the B-NiOOH (110) peak is just barely distinguishable above the radiation background. There was still noticeable quantities of Ni(OH)₂ present even in the fully charged plate. Rough indices of the level of NiOOH/Nickel were shown by the ratio of the Nickel (200) to Ni(OH)₂ (101) planes: the higher the ratio, the higher the state of charge. Since there is no reason to suspect orientation of the nickel matrix, the ratio of the two nickel lines shown gives some index of the ability of the methods used to detect orientation of any one species. Comparison of all these ratios shown (20°/23°) indicates such attempts must from necessity be very crude.

2.3.1.3 - CC#4 Test Electrode P1-27

Comparison of Nickel/Ni(OH)₂ lines indicates that this electrode was in a state of partial charge. Residual capacity of an electrode from the same cell shows that this is probably true. The ratio of the two Ni(OH)₂ lines is not appreciably different than those of the standard plates.

2.3.1.4 - CC#3 Test Electrode P1-22

The ratio of Ni/Ni(OH)₂ shows correctly that the electrode is in a high state of charge. The presence of the B-NiOOH line reaffirms this conclusion. The ratio of the two nickel lines are in about the proper range showing no unusual orientation of the matrix.

2.3.1.5 - CC#5 Test Electrode P₁-45

The ratio of Ni/Ni(OH)₂ lines shows a moderate state of charge in agreement with the residual capacities of the companion plates. The lower than expected value is due to a higher than ordinary degree of orientation of the Ni(OH)₂ (101) plane. Orientation of electrolytically formed materials is not unusual but this effect was not observed on other test plates. Most other plates were partially destroyed on the surface, however, so orientation of Ni(OH)₂ might have preceded the surface deterioration in the other plates.

2.3.1.6 - CC#9 Test Electrode P₁-75

The ratio of Nickel/Ni(OH)₂ was higher than expected from residual capacity data. This is due to loss of active material at the surface as is shown in a microphoto (Figure 6) to be described later. This was also shown by physical appearance and recharacterization data. There is no evidence of orientation of residual Ni(OH)₂ nor of the nickel matrix.

2.3.1.7 - CC#7 Test Electrode P₁-91

Ratio of Nickel/Ni(OH)₂ was higher than expected from recharacterization data indicating a surface depletion in active material. Microscopic examination (Figure 7) confirmed this. Nickel peak ratios and Ni(OH)₂ peak ratios were approximately as should be assuming no orientation.

2.3.1.8 - CC#2 Test Electrode P₁-7

The Nickel/Ni(OH)₂ ratio was higher than expected from residual capacity data. Considerable loose material adhered to the separator material however, and the photo-micrograph shows a slight depletion of active material. There was no evidence of orientation of active or conductive material.

2.3.2 - X-ray Diffraction Analysis of Negative Test Plates

Standard comparison electrodes were made in a procedure similar to that described for the positive electrodes. X-ray data is shown in Table IV. Ratios of two nickel peaks (matrix material) are assumed to show little or no orientation although the spread in ratios was somewhat greater. Two cadmium peaks had a wide spread in values which is probably due to orientation although there is no correlation between ratios and residual charge. Two cadmium hydroxide peaks had a narrower spread with no correlation with residual capacity. There seemed to be some correlation with peak heights of the strongest Cd(OH)₂/Cd peaks but it is undoubtedly spurious because of the spread in the individual material peak height ratios. Similarly, there is no information to be obtained by comparing peak heights of Nickel metal to either Cadmium or Cadmium Hydroxide peaks. Finally, there is no consistent decrease in nickel peak heights with test duration (this would have suggested extrusion of active material).

2.3.3 - X-ray Diffraction Analysis of Loose Material Adhering to Electrode Separators

When several of the CC test cells were disassembled there was considerable black material adhering to the nylon separators. The material was found to be magnetic with the bulk of it adhering to the positive electrode side of the separator. X-ray diffraction examination of separator fragments from each cell having the black residue showed strong traces of Nickel metal and Nickel Hydroxide. Surprisingly strong peaks of Cadmium and Cadmium Hydroxide were also present although there was very little dark material on the cadmium side of the separator. All samples run had approximately the same peak ratios although the individual intensities varied considerably from one sample to another.

2.3.4 Photomicrographic Study

Photomicrographs were taken of one each of the positive plates taken from each of the CC test cells except #5. The plates had previously been examined by X-ray diffraction and had been stored at room temperature in dry nitrogen prior to being photographed. All samples were in essentially the same state as when they were removed from the cycling program.

Additional pictures were taken of VO test plates which had been charged and characterized but not cycled. These were in a charged and discharged state (200 ma. for 12 hrs.) just prior to being vacuum impregnated with epoxy mounting resin and being photographed. In addition, one plate which was in the as-received condition was mounted and photographed. The results of this are described below.

The samples were vacuum impregnated with clear Bakelite ERL2795* epoxy resin and mounted in a slight incline. They were then sectioned and polished obliquely to broaden the sinter structure between the nickel-plated steel skeleton and the electrode surface. All samples were etched in 2% Nital and photographed at 100X (reduced later for reproduction). The etchant used succeeded only in defining the iron-nickel boundary of the nickel plated skeleton. Several unsuccessful attempts were made to delineate the two forms of active material such as oxidation of the Ni(II) oxide with gold chloride to precipitate gold on the discharged material. It appeared that the two nickel oxides were so intimately mixed that all such deposits were too gross to delineate differences of oxidation states but succeeded only in masking off active areas.

* A special resin which hardens without thermal spiking.

2.3.4.1 Green (as-received) VO Plaque

Figure 1 shows a sectioned green electrode. This electrode was in the as-received condition and had not been electrochemically cleaned or treated in any way. The nickel-plated steel section at the top of the photo shows a clean continuous nickel deposit on the steel skeleton of this and all other plates examined. Grain size of this and all other plates examined was ASTM-7-8.

The white material in the sintered structure is the nickel powder matrix. Grey areas are either epoxy or the active material. Boundaries between epoxy and the active material are visible as rounded or shaded lines caused by the difference in hardness of the two.

The black areas are portions of the porous matrix which were not filled by the epoxy resin. The active material was quite friable and some was lost from these areas during polishing. The distribution of the porous structure is surprisingly uniform both in size and configuration as is the distribution of the active material.

Occasional voids were seen in this and other plaques but they were generally quite small. That in the lower left portion of Figure 1, for instance, is only 18 mils (1/64"). Small micro-cracks are apparent however, and may be incipient fissures that were considerably greater in the fully charged plates (Figure 2). The thickness of the nickel plate is about 0.4 mils.

2.3.4.2 Fully Charged VO Plaque

It was reported earlier that continued overcharge condition caused blistering and pimpling of the electrode. This plate (Figure 2) received one charge cycle after electrochemical cleaning of 2400 mahrs or approximately 100% overcharge. The disruptive effect of this charging condition is shown by the large crack formation -- possibly along the incipient cracks shown in Figure 1. There are also many more macropores in the structure although these may be artifacts of the sample preparation since it is quite obvious that the sample was not fully impregnated by the epoxy. Finally there seems to be considerable attack of the nickel powder structure adjacent to the nickel plated steel skeleton.

2.3.4.3 Fully Discharge VO Plaque

Figure 3 shows the fully discharged companion electrode to that described previously. There are no gross defects visible with a very even distribution of active material and sinter structure. The thickness of nickel plate is still about 0.4 mils.

2.3.4.4. 0°C, CC#4 Test Electrode P₁-27

Only one 0°C test electrode was examined and is shown in Figure 4. The nickel plate remained at about 0.4 mil thickness over the test period (2078 cycles). The porosity seems to have increased over the test period presumably because of oxidation of the nickel powder structure. The retention of capacity on recharacterization (see Table I) indicates that the oxidized nickel was contributing to available capacity in spite of the loss of considerable material from the electrode. An interesting feature is the partial section of a pimple at the bottom of the photo. The pimple is about 30-35 mils in diameter (1/32").

2.3.4.5. 25°C, CC#3 Test Electrode P₁-22

Only one 25°C test electrodes was examined and is shown in Figure 5. There was no change in nickel plate thickness but there was gross deterioration of the powder matrix. The large pore in the center may be similar to that in Figure 1 (i.e. it may have been in the plaque originally) or it may be due to the cycling history. The presence of some nickel powder in the pore and the surface appearance (Table I) seems to indicate that it is the latter.

2.3.4.6. 40°C, CC#9 Test Electrode P₁-75

Figure 6 shows one of three 40°C test electrodes that were examined. All three 40°C test electrodes lost a considerable amount of nickel plate (estimated thickness is about 0.1 mil). This was observed only in the 40°C cells and is presumably a temperature--voltage dependent nickel corrosion. There is an obvious line of demarcation between the nickel plate and nickel powder present. This indicates a preferential corrosion of the nickel plate during the cycling test compared to that of the nickel powder. At the bottom of the photo is a sectioned pimple which is lined with a higher than ordinary amount of nickel powder. Steady accumulation of gas in pockets such as these may well be the reason for the severe deterioration of VO plates under the high C-rate characterization tests described in an earlier report. A similar pocket was seen in Figure 1 and may be the precursor of a pimple or blister.

2.3.4.7. 40°C, CC#7 Test Electrode P₁-91

The steel skeleton of this sample (Figure 7) shows some inter-granular attack adjacent to the nickel plate indicating penetration of the plate by electrolyte. The microscopic appearance of this electrode is good excepting for the effects mentioned above near the nickel plate itself. A macroscopic photo (Figure 8) shows areas evident of "crack" formation that are not visible on the photo-micrograph however. This

"cracked" appearance was observed on other plates although usually it was much less obvious.

2.3.4.8 40°C CC#2 Test Electrode P1-7

This electrode also suffered corrosion at the nickel plate as shown in Figure 9. The "island" at the bottom of the figure is the top of a pimple as is shown more clearly in Figure 10, a macrophotograph of the same sample. Considerable degradation of material is evident in both photos although the "cracks" alluded to in the previous sample are almost absent.

2.4 RA Test, Task IV

The Random Discharge Test results were not obtained this quarter. We hope to pursue electrode analysis in the final quarter in the same vein as the preceding CC test cell summary. By the end of the present quarter, the cells had 10 days of cycling underway.

2.5 RB Test -Task VII

RB test cells were not removed from the cycling tests during this quarter since primary effort was devoted to analysis of CC test cell electrodes. 120 additional have accrued to the previous numbers making a total of 358 for the 25°C cells and 166 for the 0°C and 40°C cells.

3.0 Program for Next Quarter

Examination, capacity measurements, recharacterization of test cell electrodes will be completed and conclusions reported.

4.0 New Technology Report

There were no new developments during this quarter which came under the "New Technology" clause of this contract.

TABLE I

PROGRAM TASKS

NAS 5-3477

<u>TASK</u>	<u>MEASUREMENTS</u>
1. <u>Control and Recording Equipment</u> Design and fabrication of test equipment	None
2. <u>Test Cell Assemblies</u> Design and fabrication of test cells	None
3. <u>Electrode Preparation</u> Electrochemical cleaning of reference and cell electrodes inspection and welding of identification tabs	Capacity check and weight.
4. <u>Characterization Test-CA and CB</u> C-A Constant current charging at C/10 C-B Constant current discharging at C/10	C-A Determine charge curve. Determine rate of gassing of positive electrodes. C-B Determine discharge curve.
5. <u>Shallow Discharge Cycling Tests</u> C-C. Constant current cycling to 25-35% range to determine memory effects.	C-C Make periodic capacity determination. Make analysis of physical properties. Recovery test.
6. <u>Random Discharge Tests R-A</u> Random discharges averaging 10% 25%, 50%, and 75% depth of discharge over a 6-day period using Gaussian and rectangular distribution for discharge periods.	R-A Periodic charge and discharge curve. Recharacterization tests.
7. <u>Constant Voltage, Current Limited Charging Cycling Tests R-B</u> Charge at C/5 rate and discharge at C/2 rate to 0.9 volts.	R-B Periodic charge and discharge curve. Recharacterization tests.

TABLE II - CHARACTERIZATION AND RECHARACTERIZATION DATA ON POSITIVE CC TEST ELECTRODES

Electrode No.	CC #	T°C/#Cycles	Characterization - ma hrs (Recharacterization)						Average Charge - ma hrs	Residual Capacity After CC Test - ma hrs	Physical Appearance After N Cycles	Graphitic Step - ma hrs						Nitrate Reduction Step*- ma hrs					
			1	2	3	4	5	6				1	2	3	4	5	6	1	2	3	4	5	6
P1-28	#4 C/10	0°C/2078	1190 (1170)	1170	1180	1180	1180	1190 (1040)	1182 (1139)	188	Extensive pimpling, some act. matl. lost	98 (32)	112	112	110	112	105 (88)	14	14	14	17	17	17
P1-23	#3	250°/2660	1140 (1035)	1130	1140	1140	1140	1140 (950)	1138 (1033)	1138	One large blister; pimpling	63 (24)	66	73	80	87	87	11	14	14	14	14	17
P1-24	#3	26°/2660	1050 (1075)	1050	1050	1040	1050	1050 (945)	1048 (1042)	-	Pimpling	91 (40)	98	102	105	112	116 (131)	7	10	7	7	7	7
P1-43	#5	250°/2579	1060 (1150)	1060	1060	1060	1060	1060 (1090)	1050 (1143)	230	No visible change in electrode appearance after completion of	50 (72)	75	70	75	50	80	-	10	10	10	10	10
P1-46	#5	250°/2579	1170 (1190)	1160	1060	1060	1060	1060 (1050)	1082 (1173)	317	Shallow Discharge cycling	28 (99)	67	70	73	87	92	-	-	-	-	-	-
P1-49	#5	250°/2579	1060 (1220)	1125	1125	1125	1190	1190 (1120)	1133 (1160)	263		120	200	200	180	200	200	-	-	-	-	-	-
P1-77	#9 C/3	40°/849	1230 (1170)	1140	1260	1260	1290	1230 (1030)	1235 (1123)	0	Blisters and pimpling apparent	130 (91)	130	135	144	139	126	-	-	-	-	-	-
P1-90	#7 C/10	40°/849	1270 (1270)	1300	1220	1290	1290	-	1274 (1215)	-	No visible change in appearance	110 (91)	132	132	147	158	172	14	15	16	16	15	15
P1-92	#7	40°/849	1375 (1100)	1395	1320	1385	1415	1475 (920)	1394 (1067)	363	"	116 (19)	133	131	144	150	150	10	-	10	-	0	0
P1-6	#2 C/5	40°/849	1155 (1250)	1155	1158	1158	1155	1155	1155	0	Extensively blistered, much loose black material	238 (16)	252	242	244	252	254	14	14	20	14	20	-
P1-3	#2	40°/849	1210 (1030)	1190	1190	1210	1190	1225 (990)	1203 (1060)	0	"	106 (11)	126	126	131	140	140	14	14	14	14	14	12
P-121**		40°/storage 2 mo.	1030	1050	1060	1070	1060	1060	1055		No visible change in appearance	151	158	164	168	166	171	10	10	10	14	14	14
P-122**		40°/storage "	1040	1020	1040	1030	1020	1020	1028		in appearance after 2 months storage at 40°C in air	168	160	137	154	175	175	20	17	20	18	17	18
P-123**		40°/storage "	1000	1020	1020	1040	1020	1020	1020			151	158	166	180	171	181	14	14	10	14	14	14
P-124**		40°/storage "	1060	1070	1080	1070	1060	1070	1072			140	133	120	126	154	154	14	20	20	20	18	18
P-125**		40°/storage "	940	970	960	980	970	970	965			154	161	166	168	182	172	14	10	14	10	10	10
P-126**		40°/storage "	980	980	990	980	980	980	983			154	147	123	140	168	161	14	14	10	14	17	14
P-127**		40°/storage "	990	1010	1010	1040	1020	1020	1015			140	147	151	147	165	164	14	14	14	14	14	14
P-128**		40°/storage "	1060	1060	1070	1060	1040	1050	1053			158	151	128	140	175	172	15	15	21	17	14	17
P-129**		40°/storage "	1010	1020	1040	1040	1060	1060	1038			151	154	154	168	172	172	7	14	21	17	14	17
P-130**		40°/storage "	1040	1030	1040	1040	1030	1030	1035			133	147	126	126	157	155	10	14	17	17	18	17

* "O" - no indication of nitrate reduction step.
 " - visible but not measurable indication.

** KO-15 Plates.

TABLE III - CHARACTERIZATION AND RECHARACTERIZATION DATA ON NEGATIVE CC TEST ELECTRODES

Electrode No.	CC#	T°C/#Cycles	Characterization (Recharacterization)						Average Charge (ma hrs)	% Charge Acceptance	Δ Dis Capacity (ma hrs)	Residual Capacity After CC Test - ma hrs
			1	2	3	4	5	6				
N1-26	#4 C/10	0°C/2078	chg	1680	1400	1400	1385	1385	1365	1463		781
			dis	1400	1390	1400	1390	1390	1390	1393		
			(chg)	1505	1470	1475	1445	1435	1435	(1461)	+2.8% (+40)	
N1-21	#3 C/10	25°/2660	(dis)	1490	1490	1520	1480	1360	1260	(1433)		-
			chg	1680	1420	1400	1385	1385	1370	1440		
			dis	1400	1400	1390	1290	1390	1390	1393		
N1-22	#2	26°/2660	(chg)	1380	1285	1285	1250	1245	1235	(1280)	-13.6% (-190)	-
			(dis)	1300	1240	1250	1220	1140	1070	(1203)		
			chg	1590	1400	1400	1380	1385	1385	1423		
N1-24	#3	25°/2660	dis	1390	1390	1375	1390	1385	1355	1381		1373
			(chg)	1310	1165	1155	1135	1135	1110	(1168)	-16.6% (-229)	
			(dis)	1190	1170	1180	1140	1080	-	(1152)		
N1-25	#3	25°/2660	chg	1260	1385	1400	1380	1380	1365	1362		1383
			dis	1390	1390	1385	1390	1390	1350	1383		
			(chg)	1445	1425	1390	1350	1320	1295	(1371)	-6.1% (-85)	
N1-41	#5	25°/2579	(dis)	1410	1360	1360	1310	1220	1130	(1298)		1383
			chg	1570	1380	1385	1385	1405	1372	1416		
			dis	1390	1390	1385	1385	1320	1390	1377		
N1-42	#5	25°/2579	(chg)	1510	1460	1435	1405	1365	1330	(1418)	+0.1% (+1)	-
			(dis)	1480	1440	1450	1410	1290	1200	(1378)		
			chg	920	920	950	935	935	940	933		
N1-43	#5	25°/2579	dis	1060	1060	1060	1060	1060	1060	1060		289
			(chg)	1750	1645	1625	1565	1475	1435	(1583)	+26.9% (+285)	
			(dis)	1150	1545	1385	1360	1330	1300	(1345)		
N1-44	#5	25°/2579	chg	965	940	940	935	930	935	941		312
			dis	1060	1125	1060	1060	1060	1030	1061		
			(chg)	1615	1610	1520	1445	1420	1380	(1496)	+22.5% (+239)	
N1-45	#5	25°/2579	(dis)	1400	1320	1310	1280	1260	1220	(1300)		~200
			chg	960	940	940	935	930	925	938		
			dis	750	1060	1000	940	1000	1000	962		
N1-46	#5	25°/2579	(chg)	1590	1515	1520	1505	1555	1420	(1518)	+32.5% (+313)	~200
			(dis)	1320	1310	1300	1250	1240	1230	(1275)		
			chg	965	940	935	935	935	930	940		
N1-47	#5	25°/2579	dis	810	1060	1060	1060	1060	1030	1008		~200
			(chg)	1635	1530	1530	1475	1405	1575	(1525)	+28.7% (+289)	
			(dis)	1320	1350	1320	1270	1270	1250	(1297)		

TABLE III (Cont'd)

Electrode No.	CC#	T°C/#Cycles	Characterization (Recharacterization)						Average Charge (ma hrs)	% Charge Acceptance	Δ Dis Capacity (ma hrs)	Residual Capacity After CC Test - ma hrs
			1	2	3	4	5	6				
N ₁ -72	#9	40°/849	chg	1290	1345	1140	1170	-	1236	103.0%	-2.7% (-35)	763
			dis	1405	1345	1170	1170	-	1273			
			(chg)	1525	1420	1390	1350	1285	(1374)			
			(dis)	1300	1260	1230	1210	1220	(1238)			
N ₁ -50	#7 c/10	40°/849	chg	1380	1610	1150	1150	1150	1265	87.2%	+17.7% (+195)	583
			dis	1060	1090	1090	1125	1125	1103			
			(chg)	1665	1550	1515	1500	1595	(1532)			
			(dis)	1410	1340	1290	1270	1250	(1298)			
N ₁ -10	#2 c/5	40°/849	chg	1730	1610	1555	1525	1470	1557	78.2%	+1.0% (+12)	538
			dis	1315	1275	1245	1190	1140	1218			
			(chg)	1295	1280	1260	1225	1210	(1242)			
			(dis)	1320	1280	1290	1240	1170	(1230)			
N-121		40°/storage 2 mo.	chg	1590	1500	1580	1540	1540	1561	85.2%	-7.1% (-95)	-
			dis	1340	1330	1350	1290	1340	1330			
			(chg)	1560	1405	1415	1390	1330	(1402)			
			(dis)	1280	1270	1240	1210	1210	(1235)			
N-122		40°/storage 2 mo.	chg	1560	1560	1520	1470	1475	1508	90.0%	-5.8% (-79)	-
			dis	1370	1380	1360	1380	1330	1357			
			(chg)	1610	1495	1525	1485	1425	(1491)			
			(dis)	1340	1320	1280	1250	1250	(1278)			
N-123		40°/storage 2 mo.	chg	1565	1525	1490	1470	1470	1497	89.7%	-9.9% (-133)	-
			dis	1360	1350	1340	1360	1330	1343			
			(chg)	1590	1445	1405	1355	1315	(1396)			
			(dis)	1280	1290	1230	1170	1170	(1210)			
N-124		40°/storage 2 mo.	chg	1575	1590	1565	1520	1515	1537	86.9%	-7.1% (-100)	-
			dis	1310	1330	1350	1380	1330	1335			
			(chg)	1540	1400	1425	1390	1345	(1408)			
			(dis)	1250	1260	1240	1210	1230	(1235)			

TABLE IV - X-RAY DIFFRACTION DATA FOR NICKEL CC-TEST ELECTRODES

Peak Heights - Inches from Peak to Background												
Nickel Electrode	Angle ($^{\circ}2\theta$) d-Space (\AA) Cmpd Plane (hkl)	20.0 $^{\circ}$	23.1 $^{\circ}$	15.2 $^{\circ}$	17.6 $^{\circ}$	29.3 $^{\circ}$	Peak Height Ratios				Residual Capacity (ma hrs)	
		2.04 Nickel (111)	1.77 Metal (200)	2.69 Nickel (100)	2.40 Hydroxide (101)	1.40 B-NiOON (110)	23.1 $^{\circ}$ 17.6	20 $^{\circ}$ 23	17.6 15.2			
		Fully Charged	6.5	3.5	-	0.3	0.25	11.7	1.87	-		1200
Fully Discharged		6.5	3.75	0.5	1.5	-	2.5	1.74	3.0	0		
CC #4 - 0 $^{\circ}$ C/2078 cycles P ₁ -27		5.4 $^{\circ}$	3.0	0.2	0.5	-	6.0	1.80	2.5	188		
CC #3 - 25 $^{\circ}$ C/2660 cycles P ₁ -22		3.6	2.15	-	0.30	0.20	7.15	1.68	-	1138		
CC #5 - 25 $^{\circ}$ C/2660 cycles P ₁ -45		7.05	3.50	0.15	0.70	-	5.0	2.02	4.7	230, 317, 263		
CC #9 - 40 $^{\circ}$ C/849 cycles P ₁ -75		7.4	4.25	0.40	1.10	-	3.86	1.74	2.75	0		
CC #7 - 40 $^{\circ}$ C/849 cycles P ₁ -91		8.1	4.0	0.2	0.50	-	8.0	2.03	2.5	363		
CC #2 - 40 $^{\circ}$ C/849 cycles P ₁ -7		4.9	3.2	0.35	0.80	-	4.0	1.53	2.3	0		

TABLE V - X-RAY DIFFRACTION DATA FOR CADMIUM CC-TEST ELECTRODES

Cadmium Electrode	Angle 2θ d-spacing (\AA) Compd Plane (hkl)	20.0° 2.0h Nickel (111)	23.1° 1.77 Metal (200)	17.3° Cadmium ()	14.5° Cadmium ()	13.4° Cadmium Hydroxide (100) (101)	15.9° Cadmium (101)	Peak Height Ratios			Residual Capacity (ma hrs)
								20 23	17.3 14.5	15.9 13.4	
Fully Charged		7.75	4.1	4.1	1.3	1.1	2.1	1.89	3.16	1.9	0.268
Fully Discharged		7.5	4.0	0.2	0.2	1.5	2.8	1.88	1.0	1.87	7.5
CC #4 - 0°C/2078 cycles N ₁ -27		6.0	3.4	1.9	0.7	3.0	5.0	1.77	4.28	1.67	1.58
CC #3 - 25°C/2660 N ₁ -23		2.45	1.45	5.7	1.7	1.2	2.0	1.69	3.35	1.67	0.21
CC #5 - 25°C/2660 N ₁ -45		6.1	3.45	1.8	0.7	3.6	4.5	1.77	2.58	1.73	2.0
CC #9 - 40°C/849 N ₁ -71		6.4	3.5	2.45	0.25	3.9	5.9	1.84	10	1.51	1.59
CC #7 - 40°C/849 N ₁ -49		4.8	3.2	1.1	0.3	2.8	5.8	1.50	3.66	2.07	2.54
CC #2 - 40°C/849 N ₁ -9		2.8	3.15	1.45	0.6	4.3	6.9	1.13	2.43	1.6	2.97
After Storage in N ₂		4.3	3.6	2.1	0.9	5.7	>10"	1.20	2.33	>1.76	2.71
											538

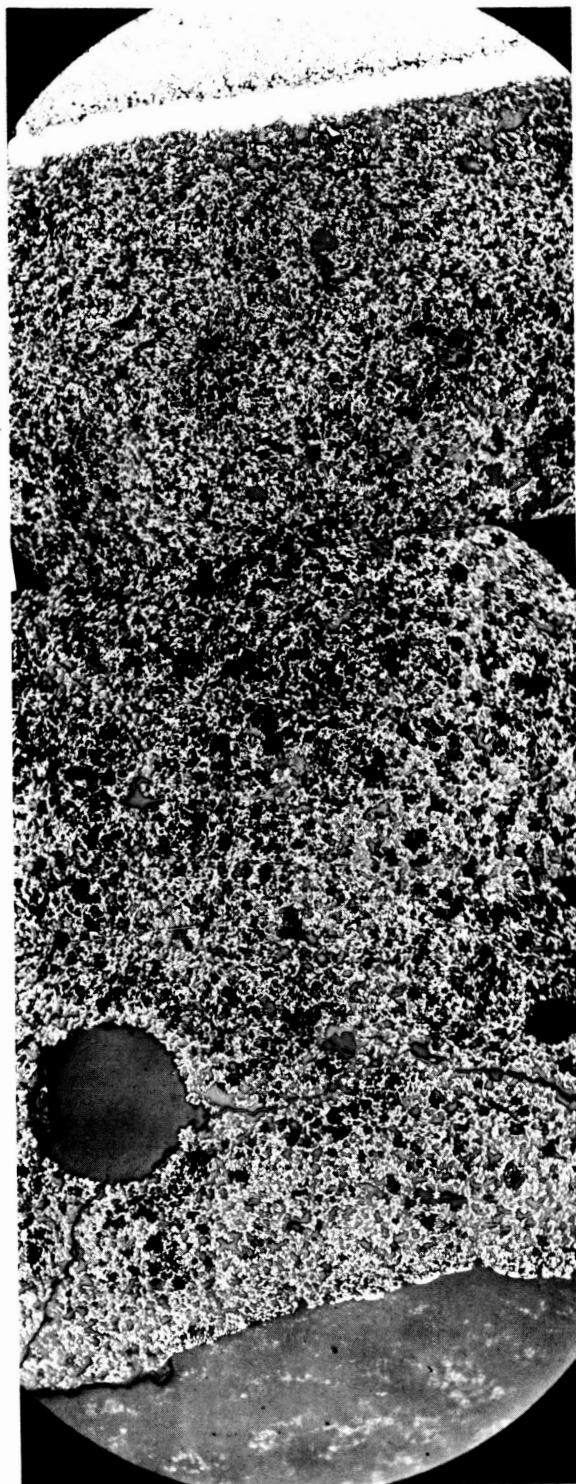


Figure 1. Green Nickel Electrode 45X 2% Nital

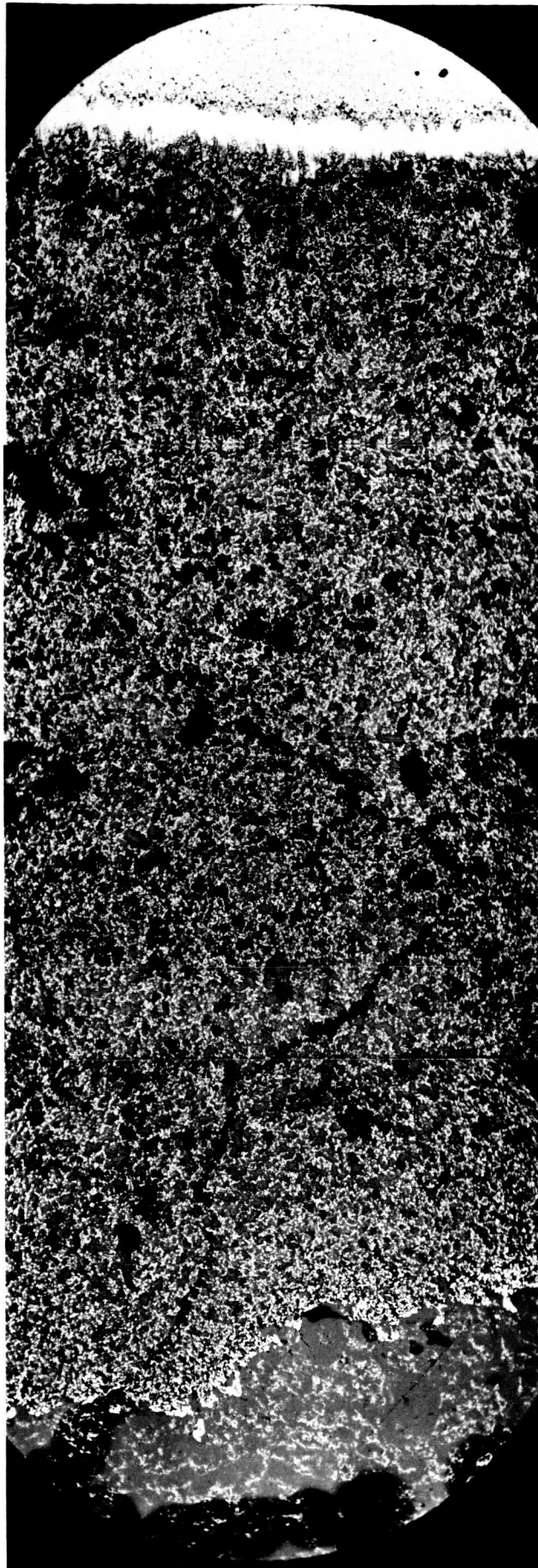


Figure 2. P5-26 45X 2% Nital (Fully charged)

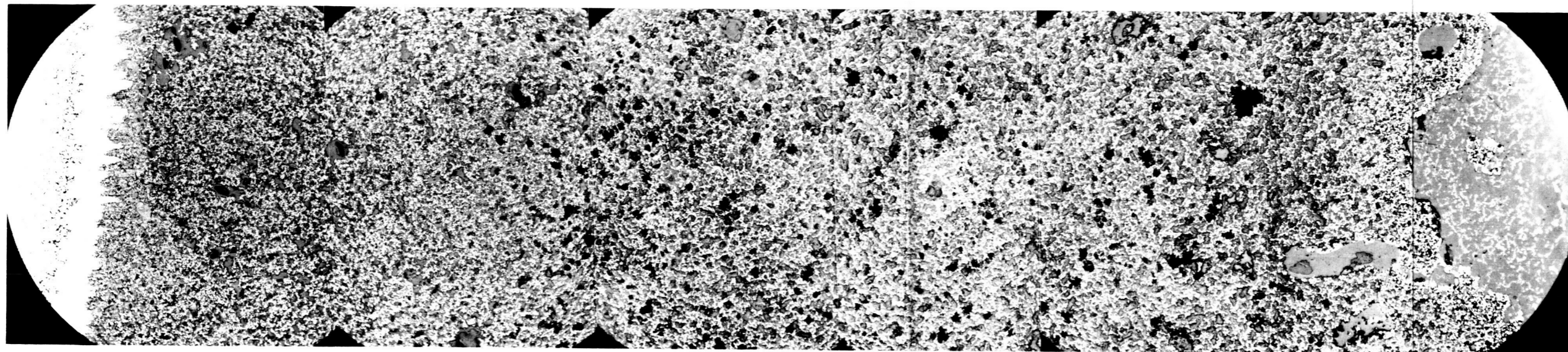


Figure 3. P5-25 45X 2% Nitral (Fully discharged)

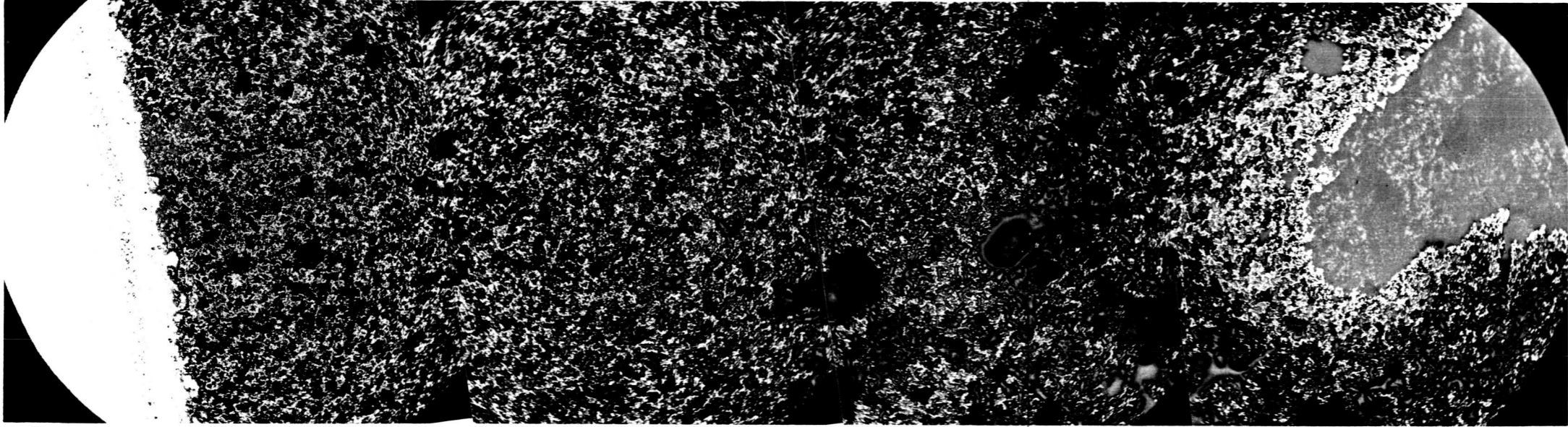


Figure 4. P1-27 45X 2% Nital

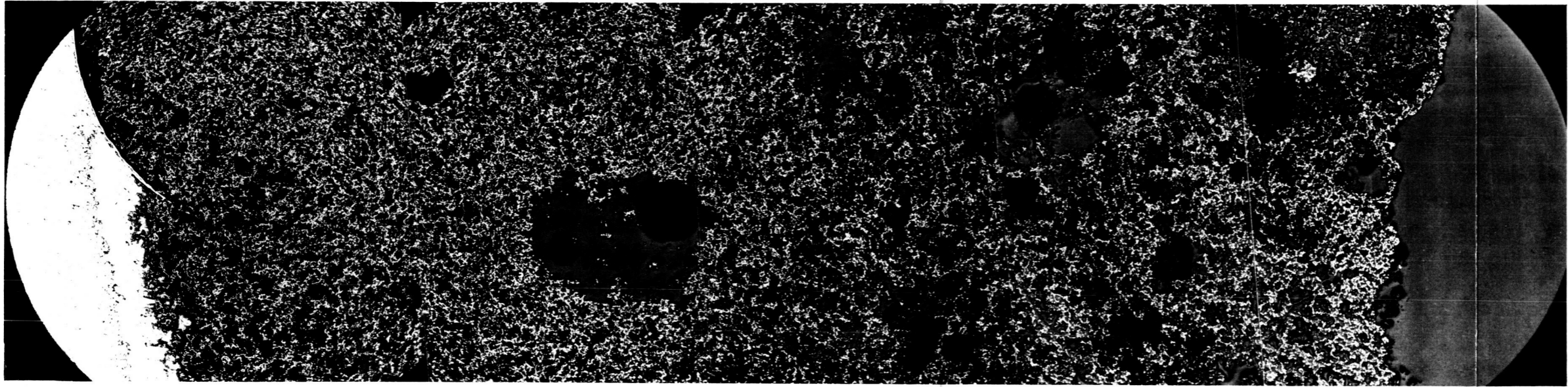


Figure 5. P1-22 45X 2% Nital

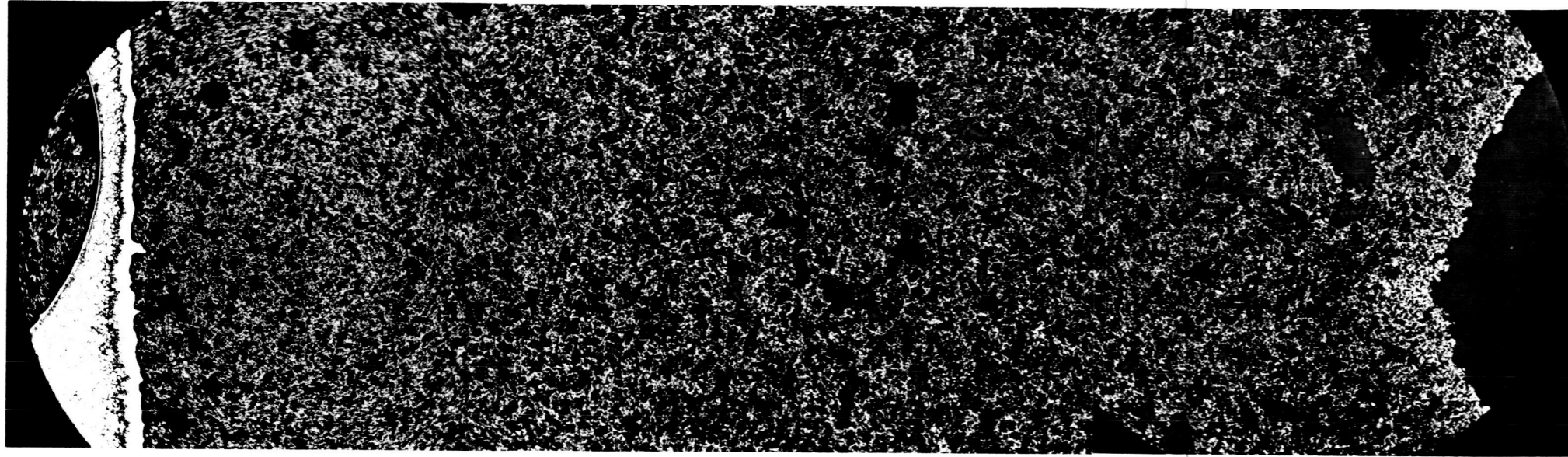


Figure 7. P1-91 45X 2% Nitral

Figure 7. P1-91 45X 2% Nitral

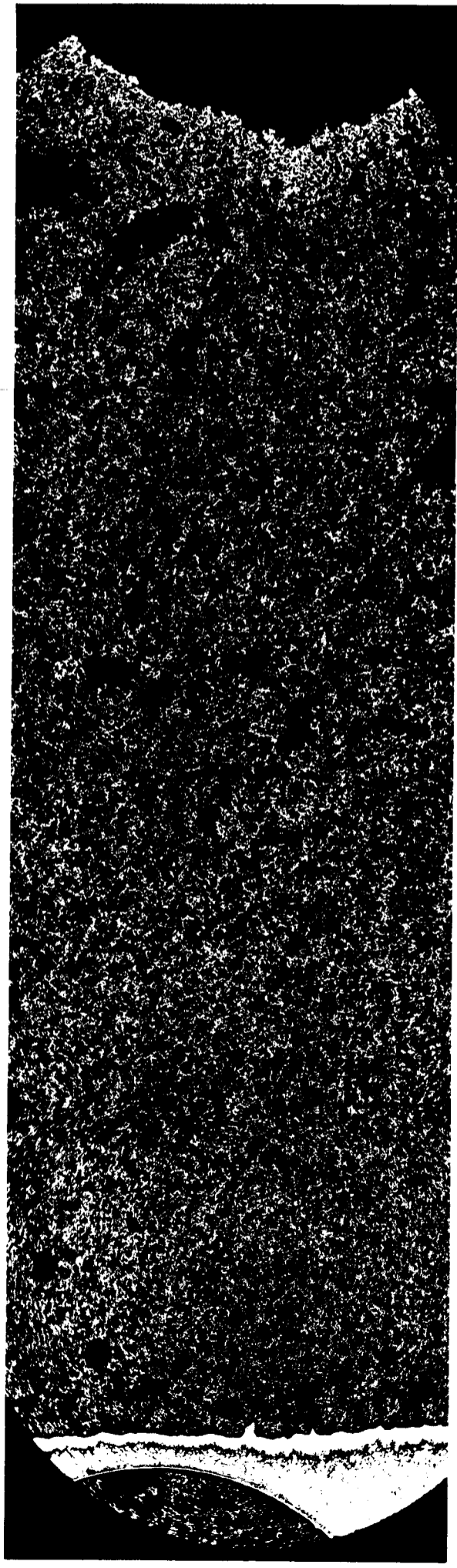
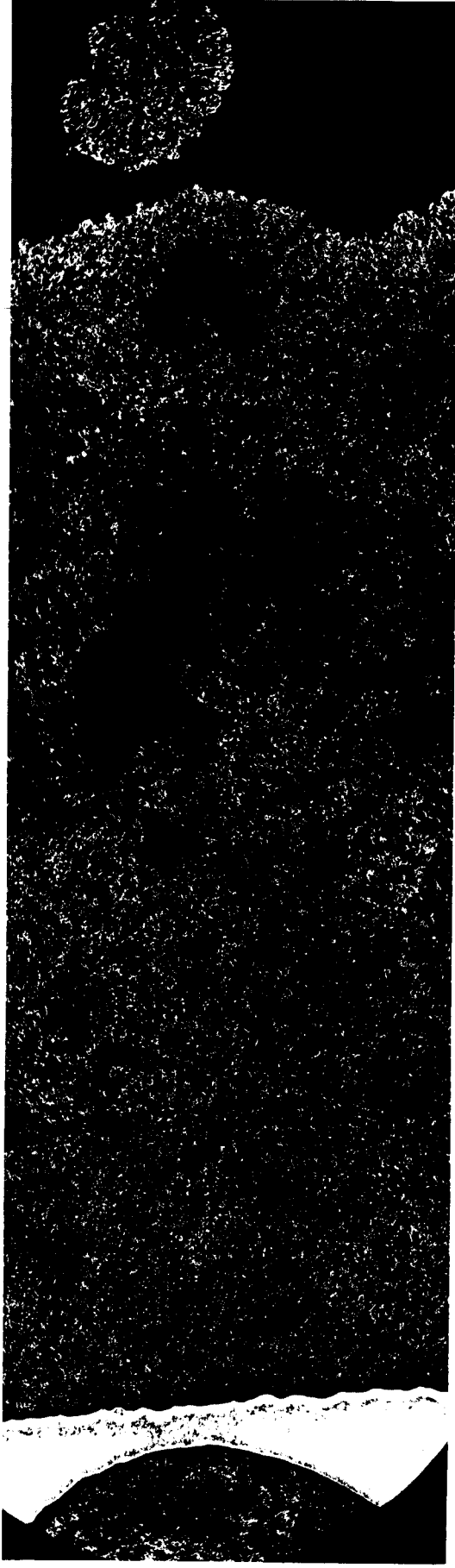




Figure 8. P1-91 5X 2% Nital

Figure 9. P1-7 45X 2% Nitral



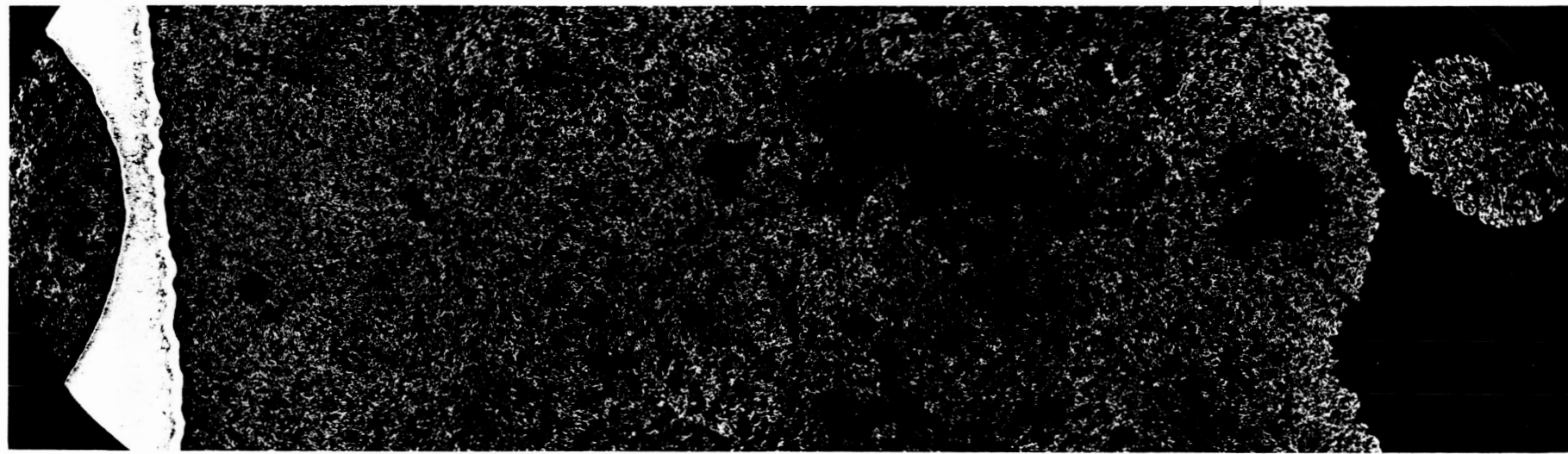


Figure 9. P1-7 45X 2% Nital